Review

Applications of BiOX in the Photocatalytic Reactions

Zhimin Yuan and Zaiyong Jiang *

School of Chemistry & Chemical Engineering and Environmental Engineering, Weifang University, Weifang 261061, China
* Correspondence: zaiyongjiang@wfu.edu.cn

Abstract: BiOX (X = Cl, Br, I) families are a kind of new type of photocatalysts, which have attracted the attention of more and more researchers. The suitable band gaps and their convenient tunability via the change of X elements enable BiOX to adapt to many photocatalytic reactions. In addition, because of their characteristics of the unique layered structure and indirect bandgap semiconductor, BiOX exhibits excellent separation efficiency of photogenerated electrons and holes. Therefore, BiOX could usually demonstrate fine activity in many photocatalytic reactions. In this review, we will present the various applications and modification strategies of BiOX in photocatalytic reactions. Finally, based on a good understanding of the above issues, we will propose the future directions and feasibilities of the reasonable design of modification strategies of BiOX to obtain better photocatalytic activity toward various photocatalytic applications.

Keywords: photocatalytic CO_2 reduction; photocatalysts; BiOX (X = Cl, Br, I); photocatalytic reactions; layer structure

1. Introduction

With the rapid development of the economy and society, the consumption of underground fossil energy, such as oil and coal, is increasing rapidly [1]. The energy crisis has gradually become the main factor restricting economic development. On the other hand, the consumption of fossil energy produces serious environmental problems, such as air and water pollution, the greenhouse effect, fog, and so on [2,3]. To deal with the energy crisis and environmental pollution, scientists worldwide are exploring a solution. Among them, semiconductor photocatalysis is a promising solution [4–10]. These semiconductor photocatalysts can absorb solar light to split H_2O to produce H_2 and O_2 gas [11], reduce carbon dioxide to organic carbon resources (such as methane, carbon monoxide, methanol, etc.) [12–14], degrade organic pollutants [15], reduce nitrogen to ammonium ion [16], reduce heavy metal ions [17], kill bacteria [18], and so on. As can be seen from the above description, photocatalysis can generate environmentally friendly clean energy only by using sunlight and solve the serious environmental pollution problem [19,20]. Therefore, it is regarded as a promising method to solve energy and environmental problems [21,22]. At present, the semiconductor photocatalysis has become a research hotspot.

Up to now, many photocatalysts have been discovered and exhibited excellent photocatalytic activities, such as TiO_2 [23], ZnO [24], ZrO_2 [25], In_2O_3 [26], BiOX [27–29], C_3N_4 [30], MOF [31], etc. Among them, BiOX (X = Cl, Br, I) families are a newly discovered type of photocatalysts, which is the crystal structure of PbFCl type (space groups P4/nmm, D_{4h} symmetry tetragonal system) [32,33]. Therefore, the BiOX crystal structure belongs to a layered type, which are composed of the staggered arrangement of the $[Bi_2O_2]^{2+}$ layer and the double X atom layer in the direction of the c-axis [34,35]. Additionally, the layers of [X-Bi-O-Bi-X] are connected by the weak van der Waals interaction [36,37]. Enough space can be provided between layers, which favors polarizing related atoms and orbitals to produce an internal electric field between the $[Bi_2O_2]^{2+}$ layer and the X atom layer. The formed internal electric field could promote the separation of photogenerated electrons

and hole pairs, which is very important for the photocatalytic activities of BiOX [38,39]. In addition, as the indirect band gap semiconductors, the photo-generated electrons derived from the valence band of BiOX need to pass a certain k-space distance to transfer the conduction band, which could lead to a low recombination rate of photon-generated carriers [40,41]. Because of their characteristics of the unique layered structure and indirect bandgap semiconductor, BiOX could usually demonstrate fine activity in many types of photocatalytic reactions.

To date, there are some review papers reported on the applications of BiOX in photocatalysis, but they are mostly focused on a particular area, such as organic degradation, CO_2 reduction, etc [42–46]. However, few of them have summarized and reported the comprehensive applications of BiOX in the whole field of photocatalysis. To make it easier and more convenient for most researchers to fully understand the applications of BiOX in photocatalytic reactions in the future, it is necessary to conduct a more comprehensive application review. In this review, we summarize relatively comprehensive recent applications of BiOX in photocatalytic reactions. We will summarize and analyze these applications in the following six fields (Table 1): BiOX split H_2O to produce H_2 and O_2 gas, degrade organic pollutants, photocatalytic nitrogen fixation, degrade the inorganics (hexavalent chromium ions), reduce carbon dioxide to organic carbon resources (such as methane, carbon monoxide, methanol, etc.), and kill bacteria. This review will be completed by presenting the mechanism of application of BiOX in each field, progress, and some modification strategies to further enhance their activities, and some current problems or challenges and future research directions.

Table 1. These photocatalytic applications of BiOX.

BiOX Six Applications in the Photocatalytic Field
Photocatalytic CO_2 reduction
Photocatalytic degrading inorganics
Photocatalytic killing bacteria
Photocatalytic N_2 fixation
Photocatalytic degrading organics
Photocatalytic splitting H_2O

2. The Difference of Band Gap among BiOX Series Photocatalysts

In photocatalytic reactions, the band gap of the photocatalyst is very important. As far as we know, the band gaps of BiOX are about 3.2 (BiOCl), 2.6 (BiOBr), and 1.7 (BiOI) eV, respectively [47]. Especially the BiOBr and BiOI, with good visible light absorption capacity, are very conducive to the efficient use of solar light in the photocatalytic reaction. Moreover, Zhao et al. [48] reported that the valence band consists mainly of O 2p and X np (Cl = 3p, Br = 4p and I = 5p, respectively), and the conduction band consists of Bi 6p states. We all know that Cl, Br, and I belong to the seventh main group elements, they should possess similar properties. Therefore, their band gaps might be conveniently tuned via the change of X elements. The suitable band gaps and convenient tunability enable BiOX to adapt to many photocatalytic reactions. Based on the previously-mentioned advantages, BiOX has attracted the attention of more and more researchers.

3. Recent Application of BiOX in the Field of Photocatalytic Reactions

3.1. Splitting H_2O to Produce H_2 and O_2

Photocatalytic splitting of H_2O began in 1972, when Fujishima and Honda discovered that H_2O molecules could be split at a titanium dioxide electrode to produce hydrogen and oxygen under the photocatalysis, making it possible to use solar energy to split H_2O into hydrogen [49]. After decades of exploration, many related photocatalysts have been discovered, such as TiO_2, ZnO, CdS, ZnS, GaN, and so on [50–54]. In recent years, BiOX photocatalysts have also been applied to split H_2O to produce hydrogen and oxygen gas, and some excellent results have been achieved [36,55–60].

The kinetic realization of the BiOX photocatalytic splitting of H_2O for hydrogen and oxygen production requires the following four processes (Figure 1) [61]: (1) absorption of photons by the BiOX photocatalyst to produce photogenerated electron-hole pairs; (2) the separation of photogenerated electron-hole pairs; (3) migration of photogenerated electrons and holes; and (4) surface chemical reactions. In other words, the electrons and holes migrating to the surface of the BiOX undergo reduction and oxidation reactions with water to produce H_2 and O_2, respectively. The chemical reaction mechanism can be simply expressed by the following reaction equation:

$$BiOX + h\upsilon \rightarrow e^- + h^+ \text{ (Semiconductor excitation and Carriers separation.)} \quad (1)$$

$$2e^- + 2H^+ \rightarrow H_2 \text{ (Half-reaction: photocatalytic hydrogen evolution.)} \quad (2)$$

$$4h^+ + 2H_2O \rightarrow O_2 + 4H^+ \text{ (Half-reaction: photocatalytic hydrogen evolution.)} \quad (3)$$

$$H_2O \rightarrow H_2 + 1/2O_2 \text{ (Total reaction: photocatalytic splitting of } H_2O.) \quad (4)$$
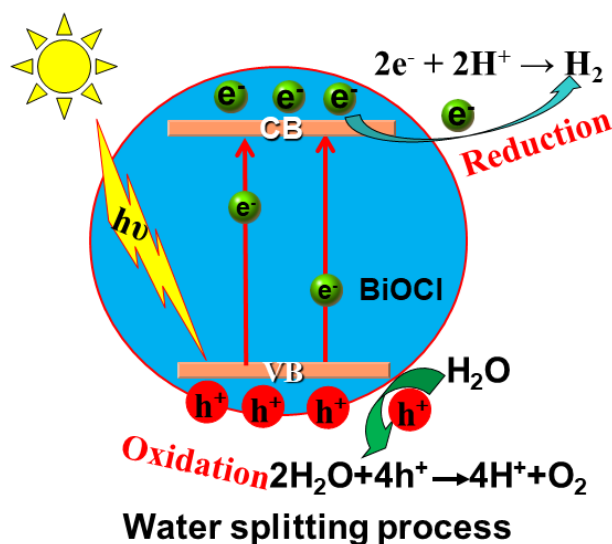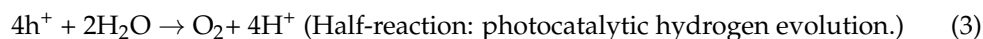

Figure 1. Schematic diagram of mechanism of the BiOCl photocatalytic splitting of H_2O.

In addition, it is important to note that for BiOX to achieve photocatalytic splitting of whole H_2O, their conduction band and valence band positions also need to meet certain requirements except having a suitable band gap. Their bottom level of the conduction band (CB) should be more negative compared to that of the redox potential of H^+/H_2 (H^+/H_2 = 0.00 V vs. SHE) [57]. On the other hand, the top level of the valence band (VB) need be more positive compared with the redox potential of O_2/H_2O (O_2/H_2O= +1.23 V, vs. SHE). However, the CB of BiOX is normally slightly more positive compared to that of H^+/H_2 potential level [61,62]. In this case, BiOX could not achieve photocatalytic splitting of H_2O for hydrogen evolution.

Because BiOX have so many advantages, researchers are looking forward to applying it to the field of photocatalytic overall water splitting. Therefore, various modification strategies for BiOX are emerging in order to realize this idea. For example, Zhang et al. prepared BiOCl nanosheets as thick as quantum sizes (obtained sample was named BOC-S) [61], which can solve the conduction band (CB) position problem of this block BiOCl. As shown in Figure 2a, the position of CB of ultrathin BOC-S upshifted by −0.3 eV than that of BOC-L (BiOCl, ~200 nm thickness)/BOC-M (BiOCl, ~30 nm thickness). There are many bismuth vacancies and oxygen vacancies exist on the surface of ultrathin BiOCl nanosheets. In the process of photocatalytic overall water splitting, H_2O adsorbed on the surfaces of BiOCl was transferred into an H atom and an OH group, subsequently, the OH group was trapped by the oxygen vacancy; On the other hand, the H atom bonds to

a surface oxygen atom. The two H atoms on the surface of BiOCl could be dissociated to produce an H_2 molecule because of the role of entropy. Finally, the ultrathin BiOCl nanosheet realized the photocatalytic overall water splitting without any sacrificial agents or co-catalysts (Figure 2b). In addition, it could be observed that both BOC-L and BOC-M did not have the photocatalytic performance of splitting H_2O. These surface defects were proved to play an important role in the whole process via the first-principles calculations. In addition, Yang et al. prepared a kermesinus BiOI (K-BiOI) with many surface oxygen vacancies [63]. They found that the position of the CB edge of K-BiOI has extended to -0.41 V vs. SHE relative to that of common BiOI (0.26 V). The CB edge is more negative than the reduction potential of H^+/H_2, thereby realizing photocatalytic H_2 production performance. To sum up, oxygen vacancy has a crucial impact on the BiOX photocatalyst to achieve photocatalytic overall water splitting.
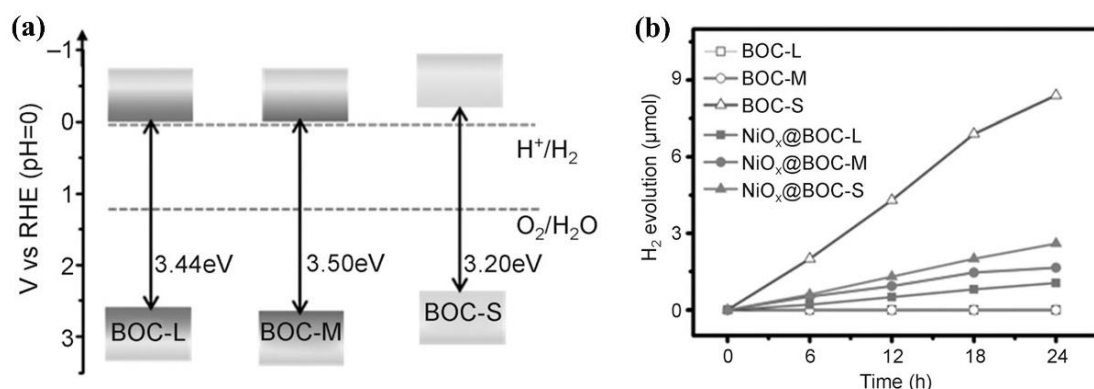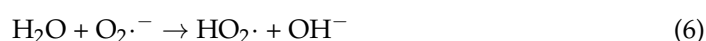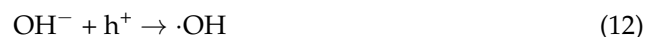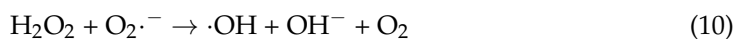

Figure 2. (**a**) Band-energy diagram of different BiOCl samples, (**b**) photocatalytic performance of splitting of H_2O over different BiOCl samples. Reprinted with permission from Ref. [61]. Copyright 2015, Wiley.

3.2. Degrading Organic Pollutants

In 1976, Carey et al. carried out pioneering work in photocatalytic degradation of organic pollutants in water [64], opening the application field of photocatalytic technology in environmental protection, and then setting off a worldwide research boom in the emerging field of semiconductor photocatalytic degradation of organics. After nearly 50 years of efforts by scientists, there have been many successful applications of semiconductor photocatalytic oxidation technology. Many experimental facts have proved that semiconductor photocatalysis can remove various organic pollutants in the environment [65–68], such as alkanes, alkenes, phenols, a variety of simple aromatic compounds, and the corresponding halides, dyes, surfactants, herbicides, pesticides, humic acids, etc.

In recent years, BiOX catalysts have attracted extensive attention for their application in photocatalytic degradation of organics due to their unique electronic structure, highly anisotropic layered structure, good photocatalytic stability, cheap, and environmentally friendly [69–71]. When BiOX degrades organic pollutants, they are first photoexcited to produce photogenerated electrons and holes. Photogenerated electrons can react with O_2 adsorbed on their surface to generate a series of free radicals with strong oxidation properties, such as $O_2 \cdot^-$, as shown in reaction Equations (5)–(10). Moreover, many photogenerated holes can directly react with H_2O molecules or OH- ions adsorbent on BiOX surface to generate $\cdot OH$ radical due to their strong oxidation ability. The reaction equation is shown in (11) and (12). Subsequently, these active free radicals with strong oxidation ability directly oxidize most organics into small inorganic molecules such as CO_2 and H_2O.

$$O_2 + e^- \rightarrow O_2 \cdot^- \tag{5}$$

$$H_2O + O_2 \cdot^- \rightarrow HO_2 \cdot + OH^- \tag{6}$$

$$2HO_2 \cdot \rightarrow H_2O_2 + O_2 \tag{7}$$

$$H_2O_2 + e^- \rightarrow \cdot OH + OH^- \tag{8}$$

$$\cdot OH + \cdot OH \rightarrow H_2O_2 \tag{9}$$

$$H_2O_2 + O_2 \cdot^- \rightarrow \cdot OH + OH^- + O_2 \tag{10}$$

$$H_2O + h^+ \rightarrow \cdot OH + H^+ \tag{11}$$

$$OH^- + h^+ \rightarrow \cdot OH \tag{12}$$

For example, Yu et al. synthesized Bi/BiOCl nanosheets via one-step solution combustion synthesis [72]. They found that Bi/BiOCl-1 showed a 98% degradation efficiency of Rhodamine B (RhB) after visible light irradiation for 120 min. Through a series of studies, they proved that not only holes can directly react with RhB on the surface of BiOCl, but also $O_2 \cdot^-$ active species could also degrade the RhB to produce CO_2 and H_2O in the photocatalytic degradation process. In addition, in the current process of BiOX degradation of organics, the catalysts are still mainly concentrated in the powder state. Therefore, the recovery and reuse of BiOX powder catalysts after use is a great challenge in practical industrial applications. Therefore, our research group designed and loaded BiOCl and BiOBr onto the surface of activated carbon fiber via a facile solvothermal method and obtained BiOCl/ACF and BiOBr/ACF samples (Figure 3) [73]. Subsequently, the photocatalytic activity on decomposing RhB and 2,4-DCP aqueous solution has been tested using BiOCl/ACF and BiOBr/ACF samples. The experimental results exhibited that they had excellent cyclic properties and stable performance. This design successfully solved the difficult problem of their recovery and reuse.
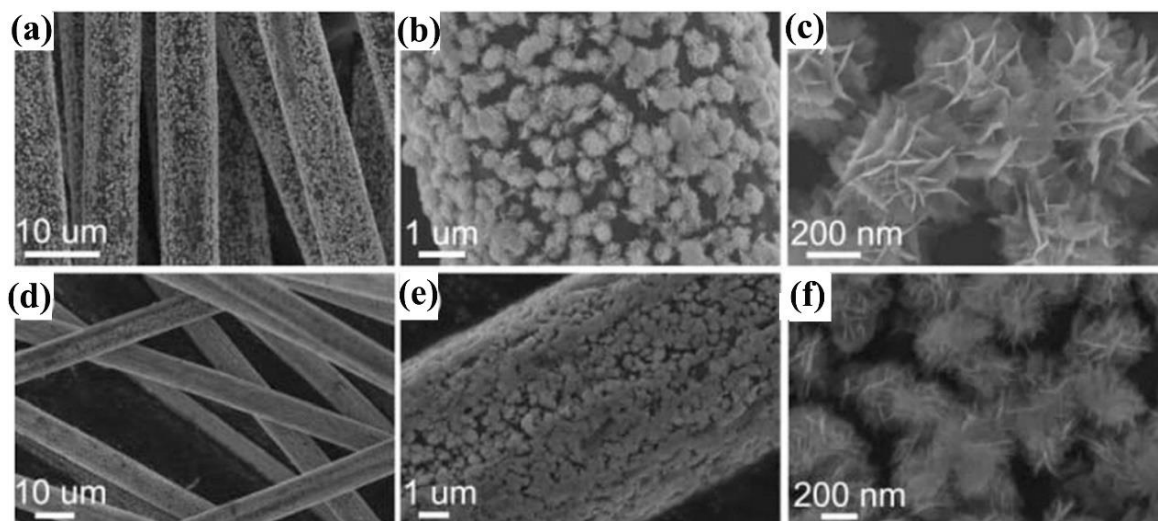

Figure 3. SEM images of BiOCl/ACF (**a**–**c**) and BiOCl/ACF (**d**–**f**). Reprinted with permission from Ref. [73]. Copyright 2015, The Royal Society of Chemistry.

Moreover, to further improve BiOX's photocatalytic degradation activity of organics, many modification strategies have been proposed, such as heterojunction, element doping, crystal plane control, etc. [74–76]. Through the continuous exploration of scientific researchers, BiOX should have relatively good activities at degrading organics. However, the corresponding industrial application technology or recycling method still needs further exploration.

3.3. Photocatalytic Nitrogen Fixation

Currently, photocatalytic nitrogen fixation is considered one of the most ideal alternatives to the traditional Haber–Bosch nitrogen fixation method. Because photocatalytic nitrogen fixation reaction is carried out at room temperature and atmospheric pressure. Moreover, nitrogen is reduced by photogenerated electrons of the photocatalyst without consuming any fossil energy. This method directly uses solar energy as energy and air and water (H_2O) as raw materials to produce ammonia gas, avoiding the disadvantages of natural gas as a feedstock for hydrogen, where hydrogen molecules can be obtained from water molecules. In addition, there is no carbon dioxide emissions in the photocatalytic nitrogen fixation, which is an ideal environmental protection nitrogen fixation technology [77–79].

In 1997, Schrauzer and Guth conducted the first photocatalytic nitrogen fixation study by using titanium dioxide photocatalysts under UV light irradiation [80]. Since then, especially in the 21st century, a lot of research work has been carried out to explore various applicable catalysts and improve the performance of photocatalysts for nitrogen reduction [81]. In the exploration process, researchers found that BiOX is a potential and promising photocatalytic nitrogen fixation catalysts. The reaction of photocatalytic reduction of nitrogen over BiOX photocatalysts can be divided into the following steps (Figure 4) [82]: (1) nitrogen adsorption, the surface-active site of BiOX to fix nitrogen; (2) BiOX uses the captured light energy to produce photogenerated electrons. The photogenerated electrons migrate to the conduction band, leaving holes in the valence band; (3) Some electrons combine with holes, and some electrons and holes migrate to the surface of the BiOX to participate in the REDOX reaction; (4) H_2O can be oxidized to produce oxygen gas via the holes, while nitrogen is reduced to ammonia after a series of multi-step injection of photogenerated electrons and water-derived protons.
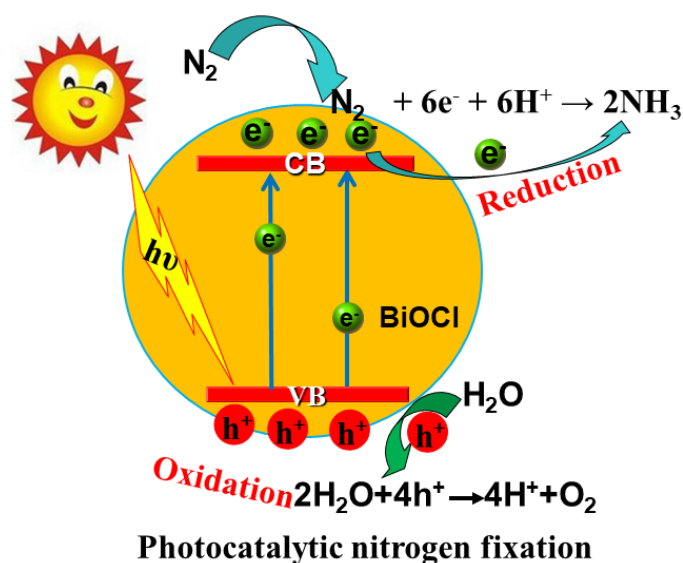

Figure 4. Schematic diagram of mechanism of photocatalytic nitrogen fixation over BiOCl photocatalytic.

In fact, pure BiOX exhibited low performance of photocatalytic nitrogen fixation. Therefore, many researchers have proposed various modification strategies to improve its catalytic activity. For example, Li et al. prepared the surface oxygen vacancies on BiOBr nanosheets, which could effectively increase the N_2 adsorption and activate the inert nitrogen molecules, while facilitating the efficient separation of photoelectrons and holes [83]. Therefore, the photocatalytic activity of nitrogen fixation was greatly improved. Xue et al. reported that the photocatalytic nitrogen fixation performance of BiOBr was improved about 10 times by the synergistic effect of oxygen vacancy and ultra-thin layer structure [84]. Gao et al. loaded the flower-like BiOBr onto the inner and outer sides of the C_3N_4 nanotubes simultaneously, effectively realizing the separation of photogenerated

electrons and hole pairs, and thus increasing the photocatalytic nitrogen fixation activity of BiOBr by 13.9 times [85]. Now, photocatalytic nitrogen fixation capacities of BiOX are still unlikely to replace the Haber–Bosch process, but their potentials are huge and need further exploration.

3.4. Degrading of Inorganics (Hexavalent Chromium Ions)

Hexavalent chromium ion (Cr(VI)) is highly toxic, easy to cause cancer, and even causes gene mutations. It cannot be biodegraded into harmless substances, resulting in enrichment in the H_2O, ultimately endangering human health [86,87]. However, trivalent chromium ions (Cr(III)) do not easily enter cells, so they are generally considered almost non-toxic. Therefore, reducing hexavalent chromium is particularly important, even imminent [88,89].

Recently, BiOX is useful for the photocatalytic reduction of hexavalent chromium ions [90,91]. In BiOX photocatalytic system, Cr(VI) has a strong oxidizing ability and could be considered an electron trapping agent, thereby being reduced by the photogenerated electrons. For example, Fan et al. prepared the BiOBr nanoflowers of high exposure (110) facets, which showed an excellent photocatalytic removal capacity for Cr(VI). The result exhibited that the whole reaction for Cr(VI) reduction was only 50 min [92]. To investigate the effect of different crystal facets of BiOCl on the photocatalytic reduction for Cr(VI) in detail, Peng et al. synthesized BiOCl with exposed (110) and BiOCl with exposed (001) facets samples (Figure 5), respectively. They found that BiOCl-110 has more excellent photoreduction activity compared to that of BiOCl-001, and 40 mL of Cr(VI) (30 mg/L) could be completely reduced within 10 min under neutral conditions [93]. To overcome the problems of insufficient light absorption capacity and low separation efficiency of photogenerated carriers, Hussain et al. prepared $BiOCl_{0.8}Br_{0.2}$ solid solution, which exhibited visible light absorption ability, a significant increase in light absorption relative to pure BiOCl [94]. At the same time, the solid solution structure is very favorable for the efficient separation of photogenic carriers. Therefore, $BiOCl_{0.8}Br_{0.2}$ exhibited a better photocatalytic reduction activity of Cr(VI) than pure BiOCl.
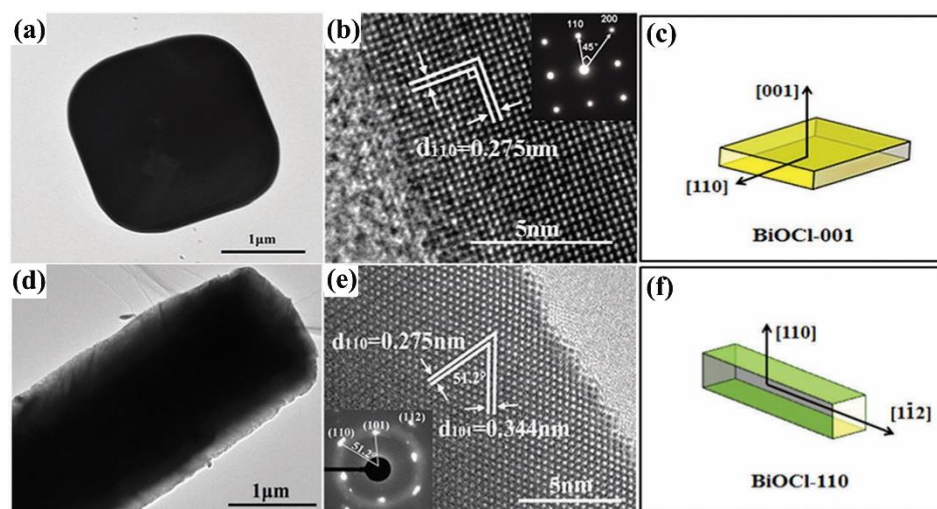

Figure 5. TEM, HRTEM images, and crystal facet models of BiOCl-001 (**a**–**c**) and BiOCl-110 (**d**–**f**). Reprinted with permission from Ref. [93]. Copyright 2018, The Royal Society of Chemistry.

In addition, to further improve the activity of BiOX photocatalytic reduction of Cr(VI), researchers have conducted a lot of exploration and research, mainly focusing on the construction of heterojunction, the construction of oxygen vacancy, doping design, etc. [95–97]. Through the review and analysis of recent studies, the BiOX series of catalysts can be considered a class of photocatalysts with good application prospects for hexavalent chromium ion treatment.

3.5. Reducing Carbon Dioxide to Organic Carbon Resources

Human activities have caused a large amount of carbon dioxide emissions, global warming is a serious problem, is also one of the most pressing challenges facing the world [98]. Over the past few decades, people worldwide have been increasingly exposed to extreme weather hazards caused by global warming, such as storms, floods, and droughts. Therefore, reducing carbon dioxide emissions, using CO_2 reuse, and achieving sustainable development have become a consensus. Harnessing solar energy to convert CO_2 into valuable chemicals and fuels is considered one of the effective solutions to global warming and energy needs [99,100].

One of the key factors affecting the activity and selectivity of photocatalysts is the separation efficiency of its photogenerated carriers in the photocatalytic CO_2 reduction process. However, conventional photocatalysts face the problem of easy recombination of photogenerated carriers, resulting in low electron transfer efficiency, so the performance of CO_2 photoreduction is not ideal. Recently, it has been shown that two-dimensional nanomaterials show good photocatalytic carrier separation efficiency when used for the photoreduction of CO_2. BiOX series photocatalysts have unique two-dimensional layered structures, which are considered promising materials for the photocatalytic reduction of CO_2. Their unique layered structures could improve the separation of photogenerated carriers and facilitates electron migration to the surface-active site, thereby accelerating the photocatalytic CO_2 reduction reaction. Therefore, carbon dioxide reduction of BiOX series photocatalysts has become a hot topic [101–103].

For example, Wu et al. prepared BiOBr atomic layers with many oxygen vacancies, which exhibited a CO generating rate of 87.4 umol g^{-1} h^{-1} in the process of visible-light-driven CO_2 reduction [104]. Via in situ FTIR and DFT calculations, they proposed a possible reaction path (Figure 6), which is as follows: (1) firstly, CO_2 and H_2O are adsorbed on the BiOBr surfaces. Subsequently, H_2O adsorbed on the BiOBr surface will be dissociated into hydrogen and hydroxy ions. CO_2 will be transferred into CO_2* active species. (2) Additionally, then, the CO_2* adsorbed BiOBr surfaces react with the surface protons, leading to the formation of a COOH* intermediate. (3) A COOH* intermediate protonation process is carried out to produce the CO* molecules. (4) The CO* active species will desorb from the BiOBr surface to form the final CO molecule. To further restrain the photogenerated electron-hole pair recombination rate and improve the product yield of BiOX photocatalysts, Sun et al. proposed to construct an effective heterojunction [105]. Therefore, they prepared an In_2O_3/BiOI composite, which showed 5.3 times higher yields of CO than those of pure BiOI. This can be attributed to forming a type II heterojunction, which promotes efficient charge separation and transfer at the heterojunction interface.

In the past few decades, researchers have made much important progress in the CO_2 reduction of BiOX photocatalytic nanomaterials. The unique layered structure of BiOX provides a good possibility for displaying excellent photocatalytic CO_2 reduction activity, but fewer active centers and low photogenerated electron transport efficiency are still not ideal. In recent years, to further improve the transport efficiency of photogenerated electrons and holes, many researchers have made BiOX into ultra-thin nanosheets and nanotubes, doped elements, and constructed surface Lewis's acid-base pairs on the surface of BiOX, and so on [106–108]. These strategies have greatly improved the photocatalytic CO_2 reduction performance of BiOX. However, there is still a huge gap between the efficiency of photocatalytic CO_2 reduction of BiOX and the actual production level, which requires further exploration and research.
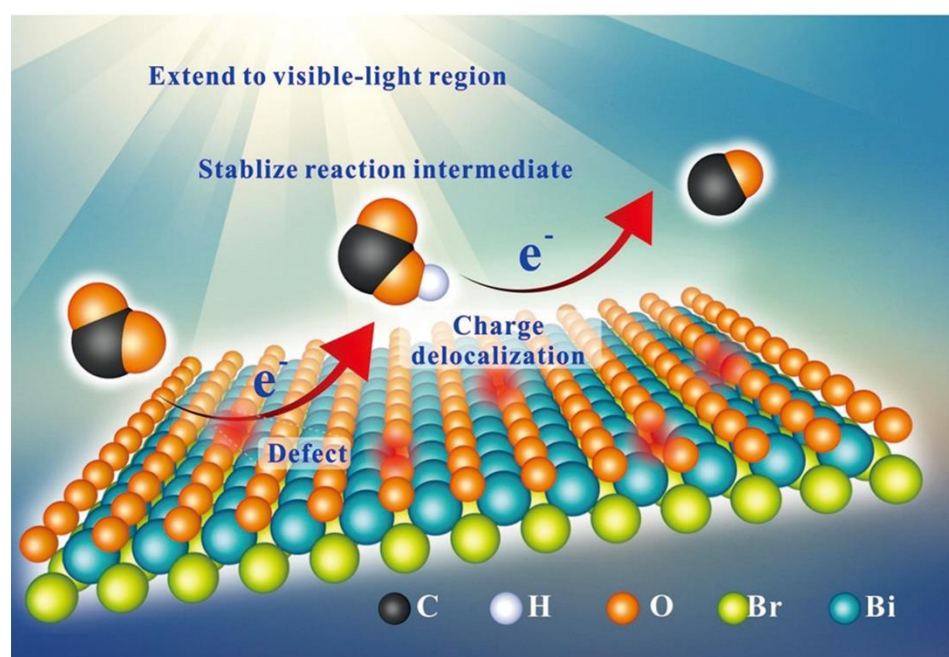
Figure 6. Schematic diagram of mechanism of CO_2 photoreduction over the BiOBr atomic layers. Reprinted with permission from Ref. [102]. Copyright 2018, Wiley.

3.6. Killing Bacteria

In our living environment, bacteria are everywhere, among which, the breeding of harmful bacteria will induce human diseases and harm human health. Therefore, how to solve harmful bacteria more effectively is a hot topic in international research. Currently, photocatalysis technology is considered a low-cost and environmentally friendly way to efficiently inactivate various bacteria [109–113]. Additionally, BiOX is a series of new types of photocatalytic materials, which is considered one of the most promising antibacterial materials due to its unique layered crystal structure, suitable band gap, high chemical stability, long-lasting antibacterial effect, low price, safety, and other advantages [114–116].

For example, Attri et al. prepared Ni-doped BiOCl nanosheets, which was observed Ni-BiOCl exhibited excellent photocatalytic antibacterial activity against *S. aureus* bacteria under visible light [117]. In the case of light conditions, the killing rate of *S. aureus* was 99.5%. They found that various active species (such as H^+, $\cdot O_2$, and $OH^{\cdot}$ generated by the Ni-BiOCl photocatalyst) encounter the surface of bacteria, and oxidize the cell wall, disturbing the cell permeability. The above-mentioned process results in the loss of intracellular components, and biomolecules, and is responsible for cell death. Our group has prepared ultrathin nanosheets of BiOI (h-BiOI) with a thickness of about 2 nm [118]. Due to the quantum size effect, the valence band of h-BiOI is a positive shift relative to the block BiOI structure, and the oxidation capacity is significantly improved. Therefore, the bactericidal capacity of h-BiOI on Escherichia coli is significantly improved compared to block BiOIs.

The bactericidal principle of BiOX series photocatalysts is as follows: a series of active species (such as h^+, $\cdot O_2^-$, H_2O_2, $\cdot OH$) are generated after performing REDOX reaction between BiOX and oxygen or water after light exposure. These active species can interact with biological macromolecules (for example, lipid, protein, enzymes, and nucleic acid macromolecules), directly or through a series of oxidative chain reactions to biological cells to cause damage, to achieve the purpose of sterilization.

4. Future Perspectives and Summary

With the rapid consumption of underground fossil energy, the energy crisis and environmental pollution are becoming more serious. Semiconductor photocatalysis is considered a very good and promising solution to solve the environmental challenge. The

key core of photocatalysis is a suitable photocatalyst. Among the many photocatalysts, the BiOX series of catalysts are considered a range of potential material due to their various advantages and was widely studied. After decades of scientific research, much research has been done to further extend the photocatalytic application field of BiOX and improve the photocatalytic efficiency of BiOX for meeting future practical processes. In this review, we summarized a relatively comprehensive six recent applications of BiOX in photocatalytic reactions. Additionally, these application mechanisms and the progress of these applications have been described briefly. Although there are decades of exploration of BiOX's various applications and these signs of progress are good, some problems or challenges need further study or optimization, thereby promoting their future practical application.

(1) In the field of photocatalytic splitting of H_2O, the conduction positions of the BiOX series of catalysts are not dominant, and it is necessary to further explore some effective ways to improve their conduction position or reduce the reduction potential through activating H_2O molecules using some modification to BiOX.

(2) Through the continuous exploration of scientific researchers, BiOX should have relatively good activities at degrading organics and hexavalent chromium ions. However, the corresponding industrial application technology or recycling method still needs further exploration. In particular, we should try to cooperate with some relatively mature methods in the industry, such as chemical treatment of pollutants, biodegradation of pollutants, etc.

(3) Now, the capacities of photocatalytic nitrogen fixation and CO_2 reduction of BiOX are still low and do not meet the actual industrial production. Therefore, further in-depth exploration and research are very necessary. Additionally, a reasonable modification strategy is very key. Reasonable modification strategies need to be designed based on reliable reaction mechanisms. Therefore, in the future, we first need to conduct a detailed exploration of the complex mechanism of photocatalytic nitrogen fixation and carbon dioxide reduction. In addition, I think it is also important to design some synergistic strategies in the process of photocatalytic CO_2 reduction, such as photothermal synergistic catalysis and the synergy of emerging surface frustrated Lewis's acid-base theory with existing modification strategies.

(4) The photocatalytic antibacterial research of BiOX series catalysts is of great significance. Photocatalytic technology can effectively avoid antibiotic resistance caused by using antibiotics. The BiOX series catalysts' recovery and lack of diffusion capacities during antibacterial use are crucial limiting factors. In future studies, we need to combine BiOX series catalysts with some suitable carriers to overcome the above problems.

References

1. Zhao, W.; Chen, Z.; Yang, X.R.; Qian, X.X.; Liu, C.X.; Zhou, D.T.; Sun, T.; Zhang, M.; Wei, G.Y.; Dissanayake, P.D.; et al. Recent advances in photocatalytic hydrogen evolution with high-performance catalysts without precious metals. *Renew. Sust. Energ. Rev.* **2020**, *132*, 110040. [CrossRef]
2. Nunes, B.N.; Lopes, O.F.; Patrocinio, A.O.T.; Bahnemann, D.W. Recent Advances in Niobium-Based Materials for Photocatalytic Solar Fuel Production. *Catalysts* **2020**, *10*, 126. [CrossRef]
3. Ma, K.; Dong, Y.; Zhang, M.; Xu, C.; Ding, Y. A homogeneous Cu-based polyoxometalate coupled with mesoporous TiO_2 for efficient photocatalytic H_2 production. *J. Colloid Interface Sci.* **2021**, *587*, 613–621. [CrossRef]
4. Jiang, Z.; Zhang, X.; Sun, W.; Yang, D.; Duchesne, P.N.; Gao, Y.; Wang, Z.; Yan, T.; Yuan, Z.; Yang, G.; et al. Building a Bridge from Papermaking to Solar Fuels. *Angew. Chem. Int. Ed.* **2019**, *58*, 14850–14854. [CrossRef] [PubMed]

5. Guo, S.; Li, X.; Li, J.; Wei, B. Boosting photocatalytic hydrogen production from water by photothermally induced biphase systems. *Nat. Commun.* **2021**, *12*, 1343. [CrossRef]

6. Chen, Z.; Yao, D.; Chu, C.; Mao, S. Photocatalytic H_2O_2 production Systems: Design strategies and environmental applications. *Chem. Eng. J.* **2023**, *451*, 138489. [CrossRef]

7. Jiang, Z.; Sun, W.; Miao, W.; Yuan, Z.; Yang, G.; Kong, F.; Yan, T.; Chen, J.; Huang, B.; An, C.; et al. Living Atomically Dispersed Cu Ultrathin TiO_2 Nanosheet CO_2 Reduction Photocatalyst. *Adv. Sci.* **2019**, *6*, 1900289. [CrossRef] [PubMed]

8. Wang, D.; Mueses, M.A.; Marquez, J.A.C.; Machuca-Martinez, F.; Grcic, I.; Peralta Muniz Moreira, R.; Li Puma, G. Engineering and modeling perspectives on photocatalytic reactors for water treatment. *Water Res.* **2021**, *202*, 117421. [CrossRef] [PubMed]

9. Chen, D.; Cheng, Y.; Zhou, N.; Chen, P.; Wang, Y.; Li, K.; Huo, S.; Cheng, P.; Peng, P.; Zhang, R.; et al. Photocatalytic degradation of organic pollutants using TiO_2-based photocatalysts: A review. *J. Clean. Prod.* **2020**, *268*, 121725. [CrossRef]

10. Jiang, Z.Y.; Miao, W.K.; Zhu, X.L.; Yang, G.H.; Yuan, Z.M.; Chen, J.C.; Ji, X.X.; Kong, F.G.; Huang, B.B. Modifying lewis base on TiO_2 nanosheets for enhancing CO_2 adsorption and the separation of photogenerated charge carriers. *Appl. Catal. B Environ.* **2019**, *256*, 117881. [CrossRef]

11. Xu, J.; Zhong, W.; Gao, D.; Wang, X.; Wang, P.; Yu, H. Phosphorus-enriched platinum diphosphide nanodots as a highly efficient cocatalyst for photocatalytic H_2 evolution of CdS. *Chem. Eng. J.* **2022**, *439*, 135758. [CrossRef]

12. Xie, Y.; Chen, J.; Wu, X.; Wen, J.; Zhao, R.; Li, Z.; Tian, G.; Zhang, Q.; Ning, P.; Hao, J. Frustrated Lewis Pairs Boosting Low-Temperature CO_2 Methanation Performance over Ni/CeO_2 Nanocatalysts. *ACS Catal.* **2022**, *12*, 10587–10602. [CrossRef]

13. Zhu, J.; Cannizzaro, F.; Liu, L.; Zhang, H.; Kosinov, N.; Filot, I.A.W.; Rabeah, J.; Bruckner, A.; Hensen, E.J.M. Ni-In Synergy in CO_2 Hydrogenation to Methanol. *ACS Catal.* **2021**, *11*, 11371–11384. [CrossRef]

14. Li, Y.; Li, B.; Zhang, D.; Cheng, L.; Xiang, Q. Crystalline Carbon Nitride Supported Copper Single Atoms for Photocatalytic CO_2 Reduction with Nearly 100% CO Selectivity. *ACS Nano* **2020**, *14*, 10552–10561. [CrossRef] [PubMed]

15. Zhang, M.; Lai, C.; Li, B.; Xu, F.; Huang, D.; Liu, S.; Qin, L.; Fu, Y.; Liu, X.; Yi, H.; et al. Unravelling the role of dual quantum dots cocatalyst in 0D/2D heterojunction photocatalyst for promoting photocatalytic organic pollutant degradation. *Chem. Eng. J.* **2020**, *396*, 125343. [CrossRef]

16. Liang, C.; Niu, H.Y.; Guo, H.; Niu, C.G.; Huang, D.W.; Yang, Y.Y.; Liu, H.Y.; Shao, B.B.; Feng, H.P. Insight into photocatalytic nitrogen fixation on graphitic carbon nitride: Defect-dopant strategy of nitrogen defect and boron dopant. *Chem. Eng. J.* **2020**, *396*, 125395. [CrossRef]

17. Li, Z.; Wang, L.; Qin, L.; Lai, C.; Wang, Z.; Zhou, M.; Xiao, L.; Liu, S.; Zhang, M. Recent advances in the application of water-stable metal-organic frameworks: Adsorption and photocatalytic reduction of heavy metal in water. *Chemosphere* **2021**, *285*, 131432. [CrossRef]

18. Baaloudj, O.; Assadi, I.; Nasrallah, N.; El Jery, A.; Khezami, L.; Assadi, A.A. Simultaneous removal of antibiotics and inactivation of antibiotic-resistant bacteria by photocatalysis: A review. *J. Water Process. Eng.* **2021**, *42*, 102089. [CrossRef]

19. Han, L.; Jing, F.; Zhang, J.; Luo, X.-Z.; Zhong, Y.-L.; Wang, K.; Zang, S.-H.; Teng, D.-H.; Liu, Y.; Chen, J.; et al. Environment friendly and remarkably efficient photocatalytic hydrogen evolution based on metal organic framework derived hexagonal/cubic In_2O_3 phase-junction. *Appl. Catal. B Environ.* **2021**, *282*, 119602. [CrossRef]

20. Zhu, X.; Wang, Y.; Guo, Y.; Wan, J.; Yan, Y.; Zhou, Y.; Sun, C. Environmental-friendly synthesis of heterojunction photocatalysts g-C_3N_4/$BiPO_4$ with enhanced photocatalytic performance. *Appl. Surf. Sci.* **2021**, *544*, 148872. [CrossRef]

21. Kumar, A.; Kumar, A.; Krishnan, V. Perovskite Oxide Based Materials for Energy and Environment-Oriented Photocatalysis. *ACS Catal.* **2020**, *10*, 10253–10315. [CrossRef]

22. Liu, X.; Zhang, Q.; Ma, D. Advances in 2D/2D Z-Scheme Heterojunctions for Photocatalytic Applications. *Sol. RRL* **2020**, *5*, 2000397. [CrossRef]

23. Zhang, X.H.; Yuan, Z.M.; Chen, J.C.; Yang, G.H.; Dionysiou, D.D.; Huang, B.B.; Jiang, Z.Y. Enhanced CO_2 photoconversion activity of TiO_2 via double effect of CoPi as hole traps and high CO_2 capture. *Catal. Today* **2020**, *340*, 204–208. [CrossRef]

24. Goktas, S.; Goktas, A. A comparative study on recent progress in efficient ZnO based nanocomposite and heterojunction photocatalysts: A review. *J. Alloys Compd.* **2021**, *863*, 158734. [CrossRef]

25. Yerli Soylu, N.; Soylu, A.; Dikmetas, D.N.; Karbancioglu-Guler, F.; Kucukbayrak, S.; Erol Taygun, M. Photocatalytic and Antimicrobial Properties of Electrospun TiO_2–SiO_2–Al_2O_3–ZrO_2–CaO–CeO_2 Ceramic Membranes. *ACS Omega* **2023**, *8*, 10836–10850. [CrossRef] [PubMed]

26. Mu, J.; Chen, B.; Zhang, M.; Guo, Z.; Zhang, P.; Zhang, Z.; Sun, Y.; Shao, C.; Liu, Y. Enhancement of the visible-light photocatalytic activity of In_2O_3-TiO_2 nanofiber heteroarchitectures. *ACS Appl. Mater. Interfaces* **2012**, *4*, 424–430. [CrossRef]

27. Cheng, S.W.; Sun, Z.H.; Lim, K.H.; Zhang, T.X.; Hondo, E.; Du, T.; Liu, L.Y.; Judd, M.; Cox, N.; Yin, Z.Y.; et al. BiOCl Nanoflowers with High Levels of Oxygen Vacancy for Photocatalytic CO_2 Reduction. *ACS Appl. Nano Mater.* **2023**, *6*, 3608–3617. [CrossRef]

28. Xu, M.L.; Jiang, X.J.; Li, J.R.; Wang, F.J.; Li, K.; Cheng, X. Self-Assembly of a 3D Hollow BiOBr@Bi-MOF Heterostructure with Enhanced Photocatalytic Degradation of Dyes. *ACS Appl. Mater. Interfaces* **2021**, *13*, 56171–56180. [CrossRef]

29. Zhou, C.; Jiang, C.; Wang, R.; Chen, J.; Wang, G. CdS Microparticles Decorated with Bi^0/BiOI Nanosheets for Visible Light Photocatalytic Hydrogen Evolution. *ACS Appl. Nano Mater.* **2021**, *4*, 4939–4947. [CrossRef]

30. Li, Y.; Ding, L.; Guo, Y.; Liang, Z.; Cui, H.; Tian, J. Boosting the Photocatalytic Ability of g-C_3N_4 for Hydrogen Production by Ti_3C_2 MXene Quantum Dots. *ACS Appl. Mater. Interfaces* **2019**, *11*, 41440–41447. [CrossRef] [PubMed]

31. Kang, M.; Yu, S.H.; Baek, K.-Y.; Sung, M.M.; Cho, S. MIL-101-NH$_2$(Fe)-Coated Nylon Microfibers for Immobilized Photocatalysts in RhB and Cr(VI) Removal. *ACS Omega* **2023**, *8*, 15298–15305. [CrossRef]

32. Lu, J.; Zhou, W.; Zhang, X.; Xiang, G. Electronic Structures and Lattice Dynamics of Layered BiOCl Single Crystals. *J. Phys. Chem. Lett.* **2020**, *11*, 1038–1044. [CrossRef] [PubMed]

33. Yang, X.; Yang, X.; Peng, Y.; Li, Z.; Yu, J.; Zhang, Y. Regulating the Built-In Electric Field of BiOBr by a Piezoelectric Mineral Tourmaline and the Enhanced Photocatalytic Property. *Ind. Eng. Chem. Res.* **2022**, *61*, 1704–1714. [CrossRef]

34. Wang, Z.; Chu, Z.; Dong, C.; Wang, Z.; Yao, S.; Gao, H.; Liu, Z.; Liu, Y.; Yang, B.; Zhang, H. Ultrathin BiOX (X = Cl, Br, I) Nanosheets with Exposed {001} Facets for Photocatalysis. *ACS Appl. Nano Mater.* **2020**, *3*, 1981–1991. [CrossRef]

35. Zhang, H.; Yang, Y.; Zhou, Z.; Zhao, Y.; Liu, L. Enhanced Photocatalytic Properties in BiOBr Nanosheets with Dominantly Exposed (102) Facets. *J. Phys. Chem. C* **2014**, *118*, 14662–14669. [CrossRef]

36. Shi, M.; Li, G.; Li, J.; Jin, X.; Tao, X.; Zeng, B.; Pidko, E.A.; Li, R.; Li, C. Intrinsic Facet-Dependent Reactivity of Well-Defined BiOBr Nanosheets on Photocatalytic Water Splitting. *Angew. Chem. Int. Ed. Engl.* **2020**, *59*, 6590–6595. [CrossRef]

37. Li, X.; Hu, Y.; Dong, F.; Huang, J.; Han, L.; Deng, F.; Luo, Y.; Xie, Y.; He, C.; Feng, Z.; et al. Non-noble-metallic Ni$_2$P nanoparticles modified O$_V$-BiOBr with boosting photoelectrochemical hydrogen evolution without sacrificial agent. *Appl. Catal. B Environ.* **2023**, *325*, 122341. [CrossRef]

38. Guan, C.; Hou, T.; Nie, W.; Zhang, Q.; Duan, L.; Zhao, X. Sn^{4+} doping enhanced inner electric field for photocatalytic performance promotion of BiOCl based nanoflowers. *Appl. Surf. Sci.* **2022**, *604*, 154498. [CrossRef]

39. Zhang, H.; Chen, X.; Zhang, Z.; Yu, K.; Zhu, W.; Zhu, Y. Highly-crystalline Triazine-PDI Polymer with an Enhanced Built-in Electric Field for Full-Spectrum Photocatalytic Phenol Mineralization. *Appl. Catal. B Environ.* **2021**, *287*, 119957. [CrossRef]

40. Zhang, K.; Liu, C.; Huang, F.; Zheng, C.; Wang, W. Study of the electronic structure and photocatalytic activity of the BiOCl photocatalyst. *Appl. Catal. B Environ.* **2006**, *68*, 125–129. [CrossRef]

41. Huang, W.L.; Zhu, Q.S. Electronic structures of relaxed BiOX (X = F, Cl, Br, I) photocatalysts. *Comput. Mater. Sci.* **2008**, *43*, 1101–1108. [CrossRef]

42. Singh, S.; Sharma, R.; Khanuja, M. A review and recent developments on strategies to improve the photocatalytic elimination of organic dye pollutants by BiOX (X = Cl, Br, I, F) nanostructures. *Korean J. Chem. Eng.* **2018**, *35*, 1955–1968. [CrossRef]

43. Hu, X.; Guo, R.T.; Chen, X.; Bi, Z.X.; Wang, J.; Pan, W.G. Bismuth-based Z-scheme structure for photocatalytic CO$_2$ reduction: A review. *J. Environ. Chem. Eng.* **2022**, *10*, 108582. [CrossRef]

44. Ahmad, I.; Shukrullah, S.; Yasin Naz, M.; Ullah, S.; Ali Assiri, M. Designing and modification of bismuth oxyhalides BiOX (X = Cl, Br and I) photocatalysts for improved photocatalytic performance. *J. Ind. Eng. Chem.* **2022**, *105*, 1–33. [CrossRef]

45. Cheng, H.; Huang, B.; Dai, Y. Engineering BiOX (X = Cl, Br, I) nanostructures for highly efficient photocatalytic applications. *Nanoscale* **2014**, *6*, 2009–2026. [CrossRef]

46. Guo, J.; Li, X.; Liang, J.; Yuan, X.; Jiang, L.; Yu, H.; Sun, H.; Zhu, Z.; Ye, S.; Tang, N.; et al. Fabrication and regulation of vacancy-mediated bismuth oxyhalide towards photocatalytic application: Development status and tendency. *Coord. Chem. Rev.* **2021**, *443*, 214033. [CrossRef]

47. Yang, Y.; Zhang, C.; Lai, C.; Zeng, G.; Huang, D.; Cheng, M.; Wang, J.; Chen, F.; Zhou, C.; Xiong, W. BiOX (X = Cl, Br, I) photocatalytic nanomaterials: Applications for fuels and environmental management. *Adv. Colloid Interface Sci.* **2018**, *254*, 76–93. [CrossRef]

48. Zhao, L.; Zhang, X.; Fan, C.; Liang, Z.; Han, P. First-principles study on the structural, electronic and optical properties of BiOX (X = Cl, Br, I) crystals. *Physica B Condens. Matter* **2012**, *407*, 3364–3370. [CrossRef]

49. Fujishima, A.; Honda, K. Electrochemical Photolysis of Water at a Semiconductor Electrode. *Nature* **1972**, *238*, 37–38. [CrossRef] [PubMed]

50. Zhu, J.M.; Zhu, S.L.; Kong, X.C.; Liang, Y.Q.; Li, Z.Y.; Wu, S.L.; Luo, S.Y.; Chang, C.T.; Cui, Z.D. Rutile-Coated B-Phase TiO$_2$ Heterojunction Nanobelts for Photocatalytic H$_2$ Evolution. *ACS Appl. Nano Mater.* **2020**, *3*, 10349–10359. [CrossRef]

51. Trang, T.N.Q.; Phan, T.B.; Nam, N.D.; Thu, V.T.H. In Situ Charge Transfer at the Ag@ZnO Photoelectrochemical Interface toward the High Photocatalytic Performance of H$_2$ Evolution and RhB Degradation. *ACS Appl. Mater. Interfaces* **2020**, *12*, 12195–12206. [CrossRef] [PubMed]

52. Chen, Y.; Wang, Z.; Zhang, Y.; Wei, P.; Xu, W.; Wang, H.; Yu, H.; Jia, J.; Zhang, K.; Peng, C. S-Scheme and Schottky Junction Synchronous Regulation Boost Hierarchical CdS@Nb$_2$O$_5$/Nb$_2$CT$_x$ (MXene) Heterojunction for Photocatalytic H$_2$ Production. *ACS Appl. Mater. Interfaces* **2023**, *15*, 20027–20039. [CrossRef] [PubMed]

53. Sun, G.T.; Shi, J.W.; Mao, S.M.; Ma, D.D.; He, C.; Wang, H.K.; Cheng, Y.H. Dodecylamine coordinated tri-arm CdS nanorod wrapped in intermittent ZnS shell for greatly improved photocatalytic H$_2$ evolution. *Chem. Eng. J.* **2022**, *429*, 132382. [CrossRef]

54. Li, J.; Yang, W.; Wu, A.; Zhang, X.; Xu, T.; Liu, B. Band-Gap Tunable 2D Hexagonal (GaN)$_{1-x}$(ZnO)$_x$ Solid-Solution Nanosheets for Photocatalytic Water Splitting. *ACS Appl. Mater. Interfaces* **2020**, *12*, 8583–8591. [CrossRef] [PubMed]

55. Jiang, Z.Y.; Liu, Y.Y.; Jing, T.; Huang, B.B.; Wang, Z.Y.; Zhang, X.Y.; Qin, X.Y.; Dai, Y. One-pot solvothermal synthesis of S doped BiOCl for solar water oxidation. *RSC Adv.* **2015**, *5*, 47261–47264. [CrossRef]

56. Lee, G.J.; Zheng, Y.C.; Wu, J.J. Fabrication of hierarchical bismuth oxyhalides (BiOX, X = Cl, Br, I) materials and application of photocatalytic hydrogen production from water splitting. *Catal. Today* **2018**, *307*, 197–204. [CrossRef]

57. Liu, Y.; Yang, B.; He, H.; Yang, S.; Duan, X.; Wang, S. Bismuth-based complex oxides for photocatalytic applications in environmental remediation and water splitting: A review. *Sci. Total Environ.* **2022**, *804*, 150215. [CrossRef]

58. Wang, J.J.; Zhang, M.; Meng, J.; Li, Q.X.; Yang, J.L. Single- and few-layer BiOI as promising photocatalysts for solar water splitting. *RSC Adv.* **2017**, *7*, 24446–24452. [CrossRef]

59. Bai, L.; Ye, F.; Li, L.; Lu, J.; Zhong, S.; Bai, S. Facet Engineered Interface Design of Plasmonic Metal and Cocatalyst on BiOCl Nanoplates for Enhanced Visible Photocatalytic Oxygen Evolution. *Small* **2017**, *13*, 1701607. [CrossRef]

60. Ning, S.B.; Shi, X.Q.; Zhang, H.W.; Lin, H.X.; Zhang, Z.Z.; Long, J.L.; Li, Y.; Wang, X.X. Reconstructing Dual-Induced {0 0 1} Facets Bismuth Oxychloride Nanosheets Heterostructures: An Effective Strategy to Promote Photocatalytic Oxygen Evolution. *Sol. RRL* **2019**, *3*, 1900059. [CrossRef]

61. Zhang, L.; Han, Z.; Wang, W.; Li, X.; Su, Y.; Jiang, D.; Lei, X.; Sun, S. Solar-Light-Driven Pure Water Splitting with Ultrathin BiOCl Nanosheets. *Chemistry* **2015**, *21*, 18089–18094. [CrossRef] [PubMed]

62. Zhao, H.; Liu, X.; Dong, Y.M.; Xia, Y.M.; Wang, H.J. A special synthesis of BiOCl photocatalyst for efficient pollutants removal: New insight into the band structure regulation and molecular oxygen activation. *Appl. Catal. B Environ.* **2019**, *256*, 117872. [CrossRef]

63. Yang, J.F.; Su, H.; Wu, Y.Y.; Li, D.G.; Zhang, D.; Sun, H.; Yin, S.Y. Facile synthesis of kermesinus BiOI with oxygen vacancy for efficient hydrogen generation. *Chem. Eng. J.* **2021**, *420*, 127607. [CrossRef]

64. Carey, J.H.; Lawrence, J.; Tosine, H.M. Photodechlorination of PCB's in the presence of titanium dioxide in aqueous suspensions. *Bull. Environ. Contam. Toxicol.* **1976**, *16*, 697–701. [CrossRef]

65. Akpan, U.G.; Hameed, B.H. Parameters affecting the photocatalytic degradation of dyes using TiO_2-based photocatalysts: A review. *J. Hazard. Mater.* **2009**, *170*, 520–529. [CrossRef] [PubMed]

66. Tang, X.; Tang, R.; Xiong, S.; Zheng, J.; Li, L.; Zhou, Z.; Gong, D.; Deng, Y.; Su, L.; Liao, C. Application of natural minerals in photocatalytic degradation of organic pollutants: A review. *Sci. Total Environ.* **2022**, *812*, 152434. [CrossRef]

67. Sano, T.; Puzenat, E.; Guillard, C.; Geantet, C.; Matsuzawa, S. Degradation of C_2H_2 with modified-TiO_2 photocatalysts under visible light irradiation. *J. Mol. Catal. A Chem.* **2008**, *284*, 127–133. [CrossRef]

68. Xie, Y.; Chang, F.; Li, C.; Chen, J.; Luo, J.; Li, L.; Hu, X. One-Pot Polyvinyl Alcohol-Assisted Hydrothermal Synthesis of Hierarchical Flower-Like BiOCl Nanoplates with Enhancement of Photocatalytic Activity for Degradation of Rhodamine B. *Clean-Soil Air Water* **2014**, *42*, 521–527. [CrossRef]

69. Su, Q.; Zhu, L.; Zhang, M.; Li, Y.; Liu, S.; Lin, J.; Song, F.; Zhang, W.; Zhu, S.; Pan, J. Construction of a Bioinspired Hierarchical $BiVO_4$/BiOCl Heterojunction and Its Enhanced Photocatalytic Activity for Phenol Degradation. *ACS Appl. Mater. Interfaces* **2021**, *13*, 32906–32915. [CrossRef] [PubMed]

70. Liu, H.; Du, C.; Li, M.; Zhang, S.; Bai, H.; Yang, L.; Zhang, S. One-Pot Hydrothermal Synthesis of SnO_2/BiOBr Heterojunction Photocatalysts for the Efficient Degradation of Organic Pollutants Under Visible Light. *ACS Appl. Mater. Interfaces* **2018**, *10*, 28686–28694. [CrossRef] [PubMed]

71. Chatterjee, A.; Kar, P.; Wulferding, D.; Lemmens, P.; Pal, S.K. Flower-Like BiOI Microspheres Decorated with Plasmonic Gold Nanoparticles for Dual Detoxification of Organic and Inorganic Water Pollutants. *ACS Appl. Nano Mater.* **2020**, *3*, 2733–2744. [CrossRef]

72. Yu, Y.; Yang, Z.X.; Shang, Z.C.; Wang, X.H. One-step solution combustion synthesis of Bi/BiOCl nanosheets: Reaction mechanism and photocatalytic RhB degradation. *J. Phys. Chem. Solids* **2023**, *174*, 111172. [CrossRef]

73. Jiang, Z.; Huang, B.; Lou, Z.; Wang, Z.; Meng, X.; Liu, Y.; Qin, X.; Zhang, X.; Dai, Y. Immobilization of BiOX (X = Cl, Br) on activated carbon fibers as recycled photocatalysts. *Dalton Trans.* **2014**, *43*, 8170–8173. [CrossRef]

74. Guo, T.Y.; Fan, X.R.; Jiang, X.Y.; Qi, Y.; Du, J.P.; Zhang, A.M.; Wang, H.T. Engineering shape of BiOCl nanosheets with improved visible-light response for superior photocatalytic degradation of Rhodamine B. *J. Alloys Compd.* **2023**, *948*, 169586. [CrossRef]

75. Wu, Z.H.; Li, W.L.; Xu, J.Y.; Jing, J.F.; Li, J.S.; Shen, J.; Yang, L.; Feng, W.H.; Zhang, S.Y.; Zhu, Y.F. Internal Electric Field Enhancement by the I-Rich Surface of Highly Crystallized BiOI Nanosheets for Boosted Photocatalytic Degradation of Phenol. *Small Struct.* **2023**, 2200380. [CrossRef]

76. Fenelon, E.; Bui, D.P.; Tran, H.H.; You, S.J.; Wang, Y.F.; Cao, T.M.; Van Pham, V. Straightforward Synthesis of SnO_2/Bi_2S_3/BiOCl-$Bi_{24}O_{31}Cl_{10}$ Composites for Drastically Enhancing Rhodamine B Photocatalytic Degradation under Visible Light. *ACS Omega* **2020**, *5*, 20438–20449. [CrossRef]

77. Chen, J.G.; Crooks, R.M.; Seefeldt, L.C.; Bren, K.L.; Bullock, R.M.; Darensbourg, M.Y.; Holland, P.L.; Hoffman, B.; Janik, M.J.; Jones, A.K.; et al. Beyond fossil fuel-driven nitrogen transformations. *Science* **2018**, *360*, eaar6611. [CrossRef]

78. Gao, X.; Wen, Y.J.; Qu, D.; An, L.; Luan, S.L.; Jiang, W.S.; Zong, X.P.; Liu, X.Y.; Sun, Z.C. Interference Effect of Alcohol on Nessler's Reagent in Photocatalytic Nitrogen Fixation. *ACS Sustain. Chem. Eng.* **2018**, *6*, 5342–5348. [CrossRef]

79. Liao, Y.; Lin, J.N.; Cui, B.H.; Xie, G.; Hu, S. Well-dispersed ultrasmall ruthenium on TiO_2(P25) for effective photocatalytic N_2 fixation in ambient condition. *J. Photochem. Photobiol. A* **2020**, *387*, 112100. [CrossRef]

80. Schrauzer, G.N.; Guth, T.D. Photolysis of Water and Photoreduction of Nitrogen on Titanium Dioxide. *J. Am. Chem. Soc.* **1977**, *99*, 7189–7193. [CrossRef]

81. Medford, A.J.; Hatzell, M.C. Photon-Driven Nitrogen Fixation: Current Progress, Thermodynamic Considerations, and Future Outlook. *ACS Catal.* **2017**, *7*, 2624–2643. [CrossRef]

82. Chen, X.Z.; Li, N.; Kong, Z.Z.; Ong, W.J.; Zhao, X.J. Photocatalytic fixation of nitrogen to ammonia: State-of-the-art advancements and future prospects. *Mater. Horizons* **2018**, *5*, 9–27. [CrossRef]

83. Li, H.; Shang, J.; Ai, Z.; Zhang, L. Efficient Visible Light Nitrogen Fixation with BiOBr Nanosheets of Oxygen Vacancies on the Exposed {001} Facets. *J. Am. Chem. Soc.* **2015**, *137*, 6393–6399. [CrossRef]

84. Xue, X.; Chen, R.; Chen, H.; Hu, Y.; Ding, Q.; Liu, Z.; Ma, L.; Zhu, G.; Zhang, W.; Yu, Q.; et al. Oxygen Vacancy Engineering Promoted Photocatalytic Ammonia Synthesis on Ultrathin Two-Dimensional Bismuth Oxybromide Nanosheets. *Nano Lett.* **2018**, *18*, 7372–7377. [CrossRef]

85. Gao, K.; Zhang, C.; Zhu, H.; Xia, J.; Chen, J.; Xie, F.; Zhao, X.; Tang, Z.; Wang, X. Unique Tubular BiOBr/g-C₃N₄ Heterojunction with Efficient Separation of Charge Carriers for Photocatalytic Nitrogen Fixation. *Chemistry* **2023**, e202300616. [CrossRef] [PubMed]

86. Teixeira, R.A.; Pereira, W.; Souza, E.S.; Ramos, S.J.; Dias, Y.N.; Lima, M.W.; de Souza Neto, H.F.; Oliveira, E.S.; Fernandes, A.R. Artisanal gold mining in the eastern Amazon: Environmental and human health risks of mercury from different mining methods. *Chemosphere* **2021**, *284*, 131220. [CrossRef]

87. Hoang, H.G.; Chiang, C.F.; Lin, C.; Wu, C.Y.; Lee, C.W.; Cheruiyot, N.K.; Tran, H.T.; Bui, X.T. Human health risk simulation and assessment of heavy metal contamination in a river affected by industrial activities. *Environ. Pollut.* **2021**, *285*, 117414. [CrossRef] [PubMed]

88. Ding, Z.; Sun, G.; Fu, F.; Ye, C. Phase transformation of Cr(VI)-adsorbed ferrihydrite in the presence of Mn(II): Fate of Mn(II) and Cr(VI). *J. Environ. Sci.* **2022**, *113*, 251–259. [CrossRef]

89. Bonola, B.; Sosa-Rodríguez, F.S.; García-Pérez, U.M.; Romero-Ibarra, I.; Henquin, E.R.; Vazquez-Arenas, J. The influence of cathode material, current density and pH on the rapid Cr(III) removal from concentrated tanning effluents via electro-precipitation. *J. Hazard. Mater. Adv.* **2021**, *2*, 100008. [CrossRef]

90. Li, T.; Zhang, G.; Lan, H.C.; Liu, H.J.; Qu, J.H. Enhanced Photoreduction of Chromium(VI) Intercalated Ion Exchange in BiOBr₀.₇₅I₀.₂₅ Layers Structure by Bulk Charge Transfer. *ACS Sustain. Chem. Eng.* **2018**, *7*, 2429–2436. [CrossRef]

91. Luo, Z.; Ye, X.; Zhang, S.; Xue, S.; Yang, C.; Hou, Y.; Xing, W.; Yu, R.; Sun, J.; Yu, Z.; et al. Unveiling the charge transfer dynamics steered by built-in electric fields in BiOBr photocatalysts. *Nat. Commun.* **2022**, *13*, 2230. [CrossRef]

92. Fan, Z.; Zhao, Y.B.; Zhai, W.; Qiu, L.; Li, H.; Hoffmann, M.R. Facet-dependent performance of BiOBr for photocatalytic reduction of Cr(VI). *RSC Adv.* **2016**, *6*, 2028–2031. [CrossRef]

93. Peng, Y.; Mao, Y.G.; Kan, P.F.; Liu, J.Y.; Fang, Z. Controllable synthesis and photoreduction performance towards Cr(VI) of BiOCl microrods with exposed (110) crystal facets. *New J. Chem.* **2018**, *42*, 16911–16918. [CrossRef]

94. Hussain, M.B.; Khan, M.S.; Loussala, H.M.; Bashir, M.S. The synthesis of a BiOClₓBr₁₋ₓ nanostructure photocatalyst with high surface area for the enhanced visible-light photocatalytic reduction of Cr(VI). *RSC Adv.* **2020**, *10*, 4763–4771. [CrossRef]

95. Yu, F.; Jin, M.; Zhang, Y.; Lei, C.; Zhou, L.; Zhu, H.; Yu, B. Visible-Light-Driven Zr-MOF/BiOBr Heterojunction for the Efficient Synchronous Removal of Hexavalent Chromium and Rhodamine B from Wastewater. *ACS Omega* **2022**, *7*, 25066–25077. [CrossRef] [PubMed]

96. Shahid, M.Z.; Mehmood, R.; Athar, M.; Hussain, J.; Wei, Y.; Khaliq, A. BiOCl Nanoplates Doped with Fe³⁺ Ions for the Visible-Light Degradation of Aqueous Pollutants. *ACS Appl. Nano Mater.* **2020**, *4*, 746–758. [CrossRef]

97. Xiong, J.; Zeng, H.Y.; Xu, S.; Peng, J.F.; Liu, F.Y.; Wang, L.H. Enhancing the intrinsic properties of flower-like BiOI by S-doping toward excellent photocatalytic performances. *J. Mater. Sci. Technol.* **2022**, *118*, 181–189. [CrossRef]

98. Fu, Z.Y.; Yang, Q.; Liu, Z.; Chen, F.; Yao, F.B.; Xie, T.; Zhong, Y.; Wang, D.B.; Li, J.; Li, X.M.; et al. Photocatalytic conversion of carbon dioxide: From products to design the catalysts. *J. CO₂ Util.* **2019**, *34*, 63–73. [CrossRef]

99. Mustafa, A.; Lougou, B.G.; Shuai, Y.; Wang, Z.J.; Tan, H.P. Current technology development for CO₂ utilization into solar fuels and chemicals: A review. *J. Energy Chem.* **2020**, *49*, 96–123. [CrossRef]

100. Chen, G.; Waterhouse, G.I.N.; Shi, R.; Zhao, J.; Li, Z.; Wu, L.Z.; Tung, C.H.; Zhang, T. From Solar Energy to Fuels: Recent Advances in Light-Driven C₁ Chemistry. *Angew. Chem. Int. Ed. Engl.* **2019**, *58*, 17528–17551. [CrossRef]

101. Zhao, X.Z.; Xia, Y.G.; Li, H.P.; Wang, X.; Wei, J.; Jiao, X.L.; Chen, D.R. Oxygen vacancy dependent photocatalytic CO₂ reduction activity in liquid-exfoliated atomically thin BiOCl nanosheets. *Appl. Catal. B Environ.* **2021**, *297*, 120426. [CrossRef]

102. Zhu, J.Y.; Li, Y.P.; Wang, X.J.; Zhao, J.; Wu, Y.S.; Li, F.T. Simultaneous Phosphorylation and Bi Modification of BiOBr for Promoting Photocatalytic CO₂ Reduction. *ACS Sustain. Chem. Eng.* **2019**, *7*, 14953–14961. [CrossRef]

103. Sun, N.C.; Zhou, M.; Ma, X.X.; Cheng, Z.H.; Wu, J.; Qi, Y.F.; Sun, Y.J.; Zhou, F.H.; Shen, Y.X.; Lu, S.Y. Self-assembled spherical In₂O₃/BiOI heterojunctions for enhanced photocatalytic CO₂ reduction activity. *J. CO₂ Util.* **2022**, *65*, 102220. [CrossRef]

104. Wu, J.; Li, X.; Shi, W.; Ling, P.; Sun, Y.; Jiao, X.; Gao, S.; Liang, L.; Xu, J.; Yan, W.; et al. Efficient Visible-Light-Driven CO₂ Reduction Mediated by Defect-Engineered BiOBr Atomic Layers. *Angew. Chem. Int. Ed. Engl.* **2018**, *57*, 8719–8723. [CrossRef] [PubMed]

105. Wang, R.; Shen, J.; Sun, K.H.; Tang, H.; Liu, Q.Q. Enhancement in photocatalytic activity of CO₂ reduction to CH₄ by 0D/2D Au/TiO₂ plasmon heterojunction. *Appl. Surf. Sci.* **2019**, *493*, 1142–1149. [CrossRef]

106. Di, J.; Chen, C.; Zhu, C.; Song, P.; Xiong, J.; Ji, M.; Zhou, J.; Fu, Q.; Xu, M.; Hao, W.; et al. Bismuth Vacancy-Tuned Bismuth Oxybromide Ultrathin Nanosheets toward Photocatalytic CO₂ Reduction. *ACS Appl. Mater. Interfaces* **2019**, *11*, 30786–30792. [CrossRef]

107. Shi, Y.; Zhan, G.; Li, H.; Wang, X.; Liu, X.; Shi, L.; Wei, K.; Ling, C.; Li, Z.; Wang, H.; et al. Simultaneous Manipulation of Bulk Excitons and Surface Defects for Ultrastable and Highly Selective CO₂ Photoreduction. *Adv. Mater.* **2021**, *33*, e2100143. [CrossRef]

108. Wang, Q.L.; Miao, Z.R.; Zhang, Y.F.; Yan, T.J.; Meng, L.P.; Wang, X.X. Photocatalytic Reduction of CO₂ with H₂O Mediated by Ce-Tailored Bismuth Oxybromide Surface Frustrated Lewis Pairs. *ACS Catal.* **2022**, *12*, 4016–4025. [CrossRef]

109. Wang, W.; Huang, G.; Yu, J.C.; Wong, P.K. Advances in photocatalytic disinfection of bacteria: Development of photocatalysts and mechanisms. *J. Environ. Sci.* **2015**, *34*, 232–247. [CrossRef]

110. Zhou, Z.; Li, B.; Liu, X.; Li, Z.; Zhu, S.; Liang, Y.; Cui, Z.; Wu, S. Recent Progress in Photocatalytic Antibacterial. *ACS Appl. Bio. Mater.* **2021**, *4*, 3909–3936. [CrossRef]

111. Ye, L.; Pelton, R.; Brook, M.A.; Filipe, C.D.; Wang, H.; Brovko, L.; Griffiths, M. Targeted disinfection of *E. coli* via bioconjugation to photoreactive TiO$_2$. *Bioconjug Chem.* **2013**, *24*, 448–455. [CrossRef] [PubMed]

112. Zhao, J.; Huang, S.; Ravisankar, P.; Zhu, H. Two-Dimensional Nanomaterials for Photoinduced Antibacterial Applications. *ACS Appl. Bio. Mater.* **2020**, *3*, 8188–8210. [CrossRef] [PubMed]

113. Tipplook, M.; Panomsuwan, G.; Sudare, T.; Teshima, K. Graphitic Carbon Nitride Nanoflakes Decorated on Multielement-Doped Carbon as Photocatalysts for Bacterial Disinfection under Visible and Near-Infrared Light. *ACS Appl. Nano Mater.* **2022**, *5*, 3422–3433. [CrossRef]

114. Ye, L.Q.; Chen, J.N.; Tian, L.H.; Liu, J.Y.; Peng, T.Y.; Deng, K.J.; Zan, L. BiOI thin film via chemical vapor transport: Photocatalytic activity, durability, selectivity and mechanism. *Appl. Catal. B Environ.* **2013**, *130–131*, 1–7. [CrossRef]

115. Hao, R.; Xiao, X.; Zuo, X.; Nan, J.; Zhang, W. Efficient adsorption and visible-light photocatalytic degradation of tetracycline hydrochloride using mesoporous BiOI microspheres. *J. Hazard. Mater.* **2012**, *209–210*, 137–145. [CrossRef]

116. Senasu, T.; Chankhanittha, T.; Hemavibool, K.; Nanan, S. Solvothermal synthesis of BiOBr photocatalyst with an assistant of PVP for visible-light-driven photocatalytic degradation of fluoroquinolone antibiotics. *Catal. Today* **2022**, *384*, 209–227. [CrossRef]

117. Attri, P.; Garg, P.; Chauhan, M.; Singh, R.; Sharma, R.K.; Kumar, S.; Lim, D.-K.; Chaudhary, G.R. Metal doped BiOCl nano-architectures (M-BiOCl, M = Ni, Mo, Cd, Co) for efficient visible light photocatalytic and antibacterial behaviour. *J. Environ. Chem. Eng.* **2023**, *11*, 109498. [CrossRef]

118. Jiang, Z.Y.; Liang, X.Z.; Liu, Y.Y.; Jing, T.; Wang, Z.Y.; Zhang, X.Y.; Qin, X.Y.; Dai, Y.; Huang, B.B. Enhancing visible light photocatalytic degradation performance and bactericidal activity of BiOI via ultrathin-layer structure. *Appl. Catal. B Environ.* **2017**, *211*, 252–257. [CrossRef]